

Towards Label-Efficient Human Matting: A Simple Baseline for Weakly Semi-Supervised Trimap-Free Human Matting

Beomyoung Kim^{1,2} Myeong Yeon Yi¹ Joonsang Yu¹ Young Joon Yoo³ Sung Ju Hwang²

NAVER Cloud, ImageVision¹

KAIST²

Chung-Ang University³

Abstract

This paper presents a new practical training method for human matting, which demands delicate pixel-level human region identification and significantly laborious annotations. To reduce the annotation cost, most existing matting approaches often rely on image synthesis to augment the dataset. However, the unnaturalness of synthesized training images brings in a new domain generalization challenge for natural images. To address this challenge, we introduce a new learning paradigm, weakly semi-supervised human matting (WSSHM), which leverages a small amount of expensive matte labels and a large amount of budget-friendly segmentation labels, to save the annotation cost and resolve the domain generalization problem. To achieve the goal of WSSHM, we propose a simple and effective training method, named Matte Label Blending (MLB), that selectively guides only the beneficial knowledge of the segmentation and matte data to the matting model. Extensive experiments with our detailed analysis demonstrate our method can substantially improve the robustness of the matting model using a few matte data and numerous segmentation data. Our training method is also easily applicable to real-time models, achieving competitive accuracy with breakneck inference speed (328 FPS on NVIDIA V100 GPU). The implementation code is available at <https://github.com/clovaai/WSSHM>.

1. Introduction

Human matting aims to recognize the precise per-pixel opacity of human regions with significantly more elaborated details than human segmentation, and it is widely used for many applications, such as image editing and background replacement. However, obtaining matte labels is extremely costly and time-consuming since the annotations must include precise boundaries of every detail, including small hair strands, as shown in Figure 1a, which can be a daunting task for human annotators.

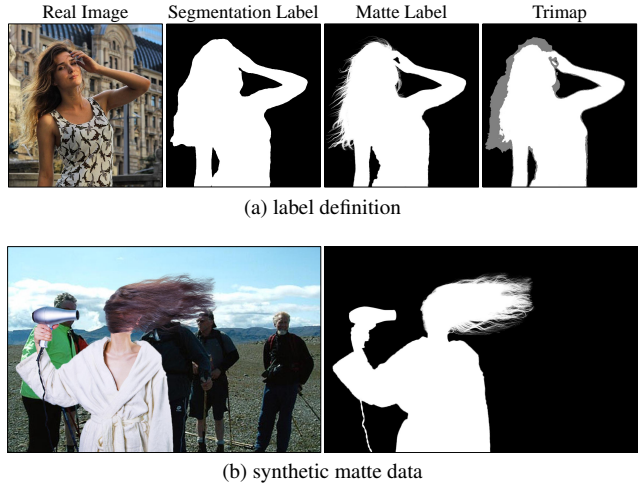


Figure 1. (a) The forms of segmentation label, matte label, and trimap. The matte label requires much more sophisticated annotations than the segmentation label. The gray-colored region in the trimap is the unknown region where details need to be estimated. (b) An example of synthetic matte data that is unnatural and lacks real-world context.

Unfortunately, publicly available matting datasets are extremely limited due to the high cost of matte annotations. For instance, Human-2K [33], Distinctions-646 [42], and DIM [54] consist of 2000, 362, and 202 images, respectively. Moreover, most of the datasets provide only foreground images. To mitigate the scarcity of labeled data, prior works [6, 19, 33, 37, 42, 54, 57, 60] utilize synthetic images to augment the datasets, as shown in Figure 1b. However, synthetic images lack the natural contextual compositions of real-world images, causing a domain generalization problem.

To circumvent this problem, previous works [6, 9, 33, 34, 37, 47, 50, 54] exploit an extra input source called trimap, which contains explicit foreground, background, and unknown region information, as shown in Figure 1a. By using the trimap as a strong prior, the solution space is reduced to the unknown (boundary) region, which is the gray-colored

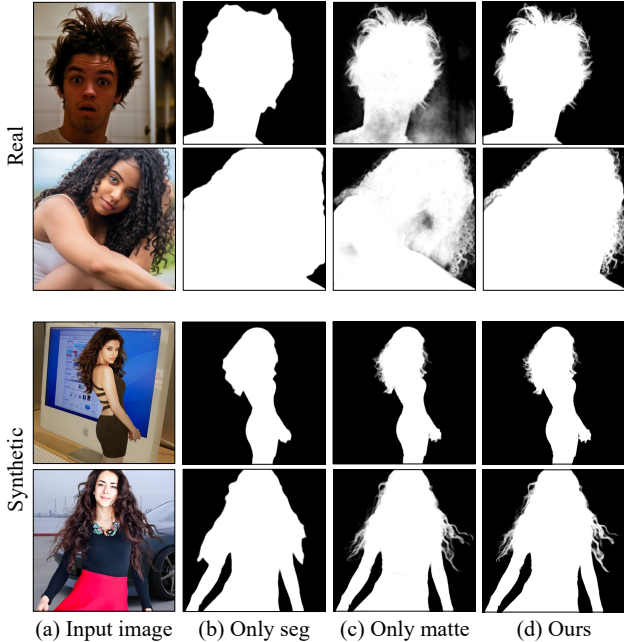


Figure 2. The qualitative comparisons of the models trained with (b) only segmentation data, (c) only matte data, (d) and both segmentation and matte data with our training method. The first and second rows are the results on natural (real-world) images, and the third and fourth rows are the results on synthetic images.

region in Figure 1a, leading to significant performance improvement on natural images even when trained with only synthetic data. However, trimap-based methods are not suitable for real-world scenarios such as real-time and non-interactive applications. To facilitate real-world applications, trimap-free approaches, which take only an image as input, have attracted more attention recently. However, when trained with only synthetic data, they often fail to generalize to natural images, as shown in Figure 2, since the absence of the trimap makes the model more vulnerable to the domain generalization problem. Building more matte data for natural images is the obvious solution, but it is not practical due to the tremendous annotation cost.

To address these challenges, we present a new learning paradigm for human matting, named **Weakly Semi-Supervised trimap-free Human Matting (WSSHM)**, to reduce the costly annotation of matte labels while improving the robustness of the trimap-free model to natural images. The WSSHM leverages a small amount of expensive matte data and a large amount of budget-friendly segmentation data, considering the segmentation label as a weak label and the matte label as a strong label, as illustrated in Figure 3. Although segmentation labels lack detailed human boundary information as shown in Figure 1a, they are significantly cheaper to obtain than matte labels and are publicly available in massive quantities for natural images. In

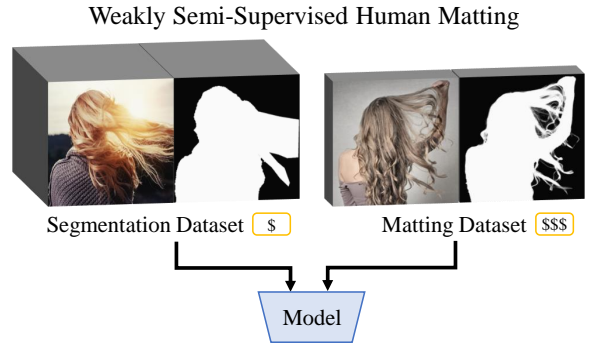


Figure 3. Illustration for the definition of Weakly Semi-Supervised Human Matting (WSSHM). The goal of the WSSHM is to train the trimap-free matting model using a small amount of expensive matte data and a large amount of economic segmentation data.

this paper, we consider that the matting dataset consists of only synthetic images and the segmentation dataset consists of only natural images, which is a realistic setting in matting research fields.

To achieve the goal of WSSHM, we introduce a baseline training strategy named **Matte Label Blending (MLB)**, which aims to maximize the synergy between segmentation and matte data in a simple and effective way. The MLB selectively leverages beneficial information from both segmentation and matte labels. Namely, segmentation data is employed to enhance the robustness of the model to natural images, and synthetic matte data is used to improve the boundary detail representation of the model.

To verify the effectiveness of the proposed method under the WSSHM setting, we precisely analyze the effect of the amount of segmentation and matte labels with extensive experiments. The results demonstrate that (1) leveraging the cost-efficient segmentation data can dramatically improve the domain generalization of the model, (2) using a small amount of matte data significantly enhances the boundary detail representation of the model, (3) the proposed method can achieve promising matte results on natural images without any matting dataset consisting of natural images, (4) our training method can be easily applicable to existing models. In summary, our contributions are as follows:

- We introduce a new learning paradigm for human matting, Weakly Semi-supervised Trimap-free Human Matting (WSSHM) to reduce annotation costs and improve domain generalization of the model to natural images.
- We propose an effective baseline method for WSSHM, named Matte Label Blending (MLB), which selectively exploits advantageous information from the matte and segmentation labels.

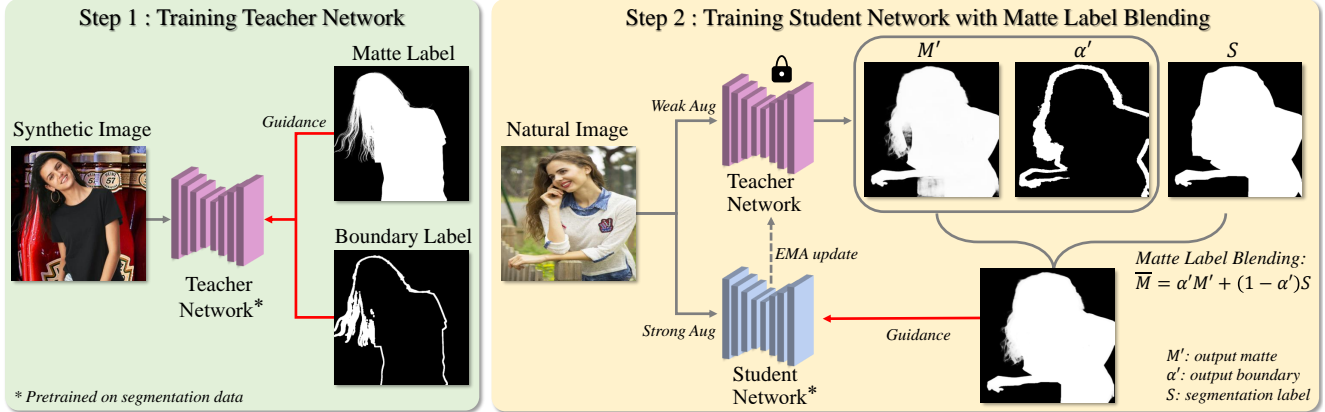


Figure 4. **Overview of the proposed training pipeline** encompassing the two-step process involving (1st step) teacher network training with synthetic matte data and (2nd step) student network training with natural segmentation data, along with the integration of Matte Label Blending (MLB) mechanism to combine boundary detail representation and domain generalization to achieve the goal of WSSHM.

2. Related Work

2.1. Human Matting

Compared to human segmentation, human matting requires detailed pixel-level estimation of the opacity of the human region. Due to the challenging nature of the matting task, most existing methods [6, 9, 33, 34, 47, 50] have employed a trimap as an auxiliary input source to focus on only the boundary region and achieve promising matte results. DIM [54] proposed an encoder-decoder network with a sequential refinement stage. MatteFormer [37] adopts the vision transformer architecture [12] and leverages the trimap as the prior token of the transformer. Additionally, some works [40, 57] utilize a coarse segmentation mask as a form of trimap. However, the necessity of obtaining the trimap (or segmentation mask) in the input space demands extra annotations or user interaction, limiting its practical applicability in real-world scenarios and real-time applications.

For the better real-world applicability, trimap-free methods [19, 32, 42, 60, 62] have been proposed. LFM [60] proposed a dual-decoder network for foreground and background identification with a fusion module. MODNet [19] presented a real-time portrait matting model that consists of three interdependent branches with a series of sub-objectives. However, due to the absence of the trimap, their performance still lags behind trimap-based methods.

BSHM [32] incorporates segmentation labels to boost matting performance, but they require three sequential sub-networks and lack detailed analysis of performance variation with the amount of segmentation and matte data. In contrast, our training method is more straightforward and flexibly applicable to existing real-time models, and we provide in-depth analyses of this synergy between the amount of segmentation and matte data.

2.2. Weakly Semi-Supervised Learning

In the field of object detection, there exist several approaches [4, 14, 22, 55, 58] to minimize annotation costs and achieve reasonably strong performance by utilizing a few amounts of fully-labeled data (*i.e.*, bounding boxes) and numerous weakly-labeled data (*e.g.*, image-level or point labels), known as weakly semi-supervised object detection. Inspired by this learning paradigm, we present weakly semi-supervised human matting (WSSHM), which considers the segmentation label as the weak label and the matte label as the strong label, to reduce annotation costs while achieving robust matting results.

3. Proposed Method

3.1. Problem Setting

Due to the high cost of annotating matte labels and the limited availability of public matting datasets, existing human matting methods [19, 37, 42, 57, 60] heavily rely on synthetic datasets. However, models trained solely on synthetic data often fail to generalize to natural images due to the lack of natural compositions in synthetic images (Figure 2c).

To address both annotation cost and domain generalization issues, we rethink the potential of coarse segmentation data in human matting. Segmentation labeling is less expensive than matte labeling, and there is a large amount of publicly available segmentation labels for natural images. In this paper, we introduce a new learning paradigm for cost-efficient trimap-free human matting, called weakly semi-supervised human matting (WSSHM), to reduce annotation cost using a small number of expensive matte labels and a large number of economical segmentation labels, while improving generalization performance to natural images.

3.2. Notation

We denote a segmentation dataset as \mathcal{D}_s that consists of a set of pairs (I^s, S) where $I^s \in \mathbb{R}^{H \times W \times 3}$ is a natural image and $S \in \{0, 1\}^{H \times W}$ is a coarse segmentation label and a matting dataset as \mathcal{D}_m that consists of a set of pairs (I^m, M) where $I^m \in \mathbb{R}^{H \times W \times 3}$ is a synthetic image and $M \in [0, 1]^{H \times W}$ is a fine matte label. The images in \mathcal{D}_s and \mathcal{D}_m are totally disjoint. Here, the I^m is composited with a foreground image I^{fg} and a background image I^{bg} as follows:

$$I^m = M \cdot I^{fg} + (1 - M) \cdot I^{bg}. \quad (1)$$

We assume that matting datasets consisting of natural images are unavailable for training, as is the case in real-world scenarios.

3.3. Baseline Training Method

We introduce a simple baseline method to achieve the goal of the WSSHM. As illustrated in Figure 4, we employ a two-step pipeline involving teacher-student networks [2, 7, 51] to effectively blend the boundary detail representation from matte data with the domain generalization capability from segmentation data.

Step 1: Teacher Network Training In the first step, we train the teacher network $f^t(\cdot)$ using the synthetic matting dataset \mathcal{D}_m to develop robust boundary detail representation. The teacher network generates two outputs: the output matte $M' \in [0, 1]^{H \times W}$ and the output boundary $\alpha' \in \{0, 1\}^{H \times W}$. The boundary label indicates regions that require detailed representation, and the ground-truth boundary label α is obtained from the matte label M in \mathcal{D}_m :

$$\alpha_{i,j} = \begin{cases} 1 & \text{if } 0.05 < M_{i,j} < 0.95 \\ 0 & \text{otherwise.} \end{cases}$$

We train the network leveraging a conventional matte loss function:

$$L = L_{matte} + \lambda L_{boundary} \quad (2)$$

$$L_{matte} = L_{mse} + L_{grad} \quad (3)$$

$$L_{mse} = (M - M')^2 \quad (4)$$

$$L_{grad} = |\nabla_x(M) - \nabla_x(M')| + |\nabla_y(M) - \nabla_y(M')| \quad (5)$$

$$L_{boundary} = |\alpha - \alpha'|, \quad (6)$$

where λ is set to 0.01 by default.

Step 2: Student Network Training with Matte Label Blending

In the second step, we freeze the teacher network and train the student network $f^s(\cdot)$ using the natural segmentation dataset \mathcal{D}_s to mitigate the domain generalization problem. The frozen teacher network provides

pseudo matte M' and boundary α' labels for the weakly augmented natural images. However, the teacher network often struggles to generalize to natural images due to the synthetic nature of the training data, as shown in Figure 2c and Figure 5b. Notably, we observe that errors primarily occur in the foreground and background regions, while predictions on the boundary regions are relatively accurate. Based on this observation, we introduce an effective label blending mechanism, named **Matte Label Blending (MLB)**. This mechanism adaptively combines the boundary representation from M' with the coarse-level knowledge from segmentation label S , generating a blended matte label $\bar{M} = \alpha' M' + (1 - \alpha') S$. Namely, as shown in Figure 5e, it removes noisy errors in the non-boundary region of M' using segmentation label S while maintaining detailed representation in the boundary region of M' , resulting in high-quality pseudo matte labels.

The student network takes strongly augmented natural images and is trained using the blended matte label \bar{M} with the L_{matte} loss function, enabling it to develop robustness to natural images and precise boundary detail representation. Additionally, we employ exponential moving average (EMA) updates to slowly update the teacher network parameters using those of the student network if both network architectures are the same. This approach effectively combines the strengths of synthetic matte data and natural segmentation data, providing a comprehensive solution for the WSSHM that improves both boundary detail representation and domain generalization.

4. Experiments

4.1. Datasets and Evaluation Metrics

Training Dataset. For the human matting dataset, we use Human-2K dataset [33], which contains 2,000 images and is publicly available. Note that images in the Human-2K dataset have only foreground region information. Following the common practice [19, 37, 42, 57, 60], we generate the synthesized images by compositing the foreground images of Human-2K dataset with background images of the COCO dataset [30], which contain no humans to prevent their negative influence on the stable training of trimap-free matting models. For the human segmentation dataset, we assemble public portrait segmentation datasets [1, 18, 46, 53]. Note that all images in the segmentation datasets are natural images. We set the maximum number of segmentation labels to 50K, and the rest of the samples, except the public datasets, are collected from our private segmentation dataset.

Validation Dataset. To validate the human matting performance, we use three matting datasets which consist of natural images (P3M [24], PPM [19], and RWP [57]) and

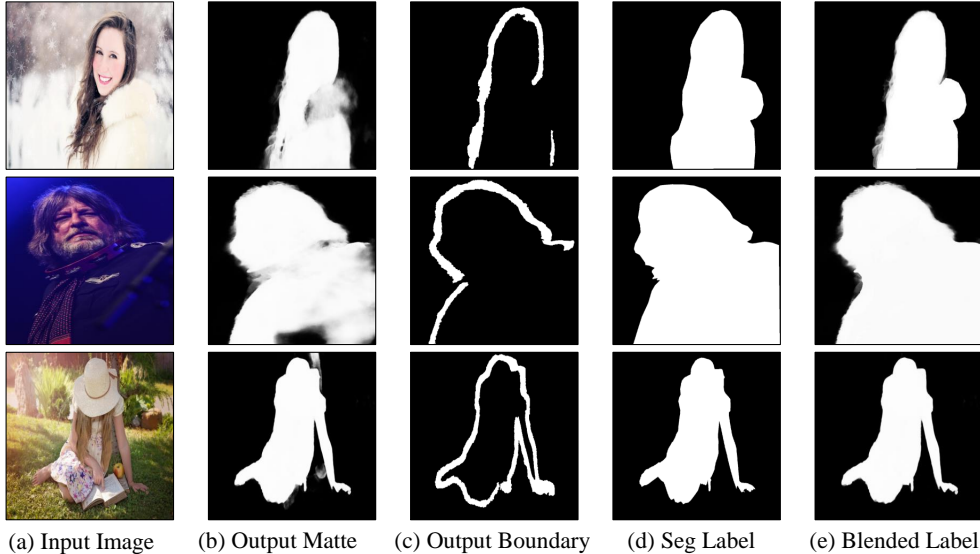


Figure 5. **Qualitative samples of Matte Label Blending** demonstrating its ability to generate high-quality blended matte labels by effectively combining boundary detail representation from teacher network outputs with the coarse-level knowledge from ground-truth segmentation labels.

one synthetic dataset (D-646 [42]). The P3M, PPM, and RWP consist of 500, 100, and 636 natural scene images. The D-646 dataset includes 362 foreground images, and we composed these foreground images with five VOC [13] background images.

Evaluation Metrics. We adopt the mean square error (MSE) and the sum of absolute differences (SAD) metrics, which are widely used for the human matting task. For the detailed analysis, we separately measure the scores on the whole and boundary regions. The pixels that are larger than 0.05 and smaller than 0.95 in the ground-truth matte label are treated as the boundary region pixels, following [57]. We mainly use the MSE metric for analysis and provide the SAD scores in the appendix.

4.2. Implementation Details

Baseline Network. We employ the U-Net [43] architecture with ResNet [16] backbone and an Atrous Spatial Pyramid Pooling [5] module as a baseline matting network, which is commonly used in existing matting approaches [6, 33, 57, 60] and quite straightforward architecture. We use the U-Net with ResNet-101 backbone for the teacher and student networks by default. The student network can be flexibly replaced with other networks. To verify the applicability of our training method on real-time models, we also adopt the ResNet-18 or ResNet-18 with a width multiplier of 0.5 backbones for the student network.

Optimization. We use the Adam optimizer, cosine learning rate decay scheduling, and a batch size of 16 to train the network. We initialize the parameters of both teacher and student networks with the pre-trained weights, which are trained on segmentation datasets, for fast and stable convergence. Note that the pre-trained weights are not used when training the model using only the matting dataset. During the pre-training stage, we set the learning rate to $1e-4$ and training iterations to 200K using the MSE objective function. The teacher network is fine-tuned on the synthetic matting dataset, the learning rate is set to $5e-5$, and the training iteration is 10K with the objective function of Eq. 3. After training the teacher network, we train the student network using the natural segmentation dataset with the Matte Label Blending strategy. Here, we set the learning rate to $5e-5$ and training iterations to 20K. We employ random scaling, random cropping, and random horizontal flipping for basic data augmentation and apply the color jittering operations [7] only for strong augmentation. We also adapt the multi-scale training strategy by cropping the image from 512×512 to 768×768 . Note that our final result is generated only from the student network. During the test time, we resize the image to the shorter edge length of the image to be 512. We train the models on 4 NVIDIA V100 GPUs using Pytorch [41] framework.

4.3. Results

We conducted extensive experiments on the proposed method to analyze the effect of varying amounts of matte and segmentation labels. We split segmentation data into six subsets with 0, 2K, 5K, 10K, 20K, and 50K labels, and

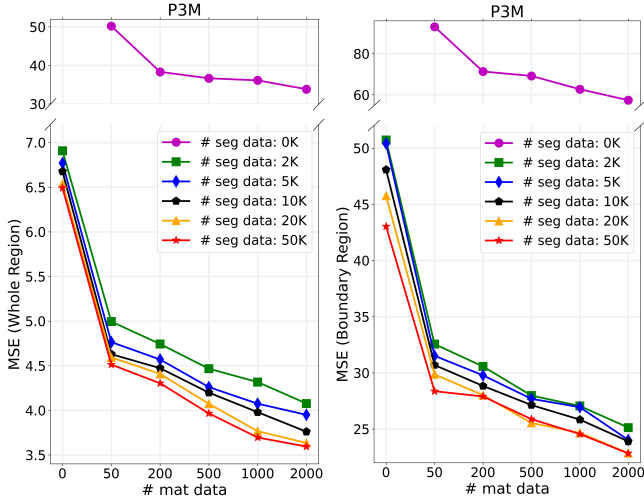


Figure 6. Comparisons on **P3M** dataset (**natural images**) according to the amount of segmentation and matte data.

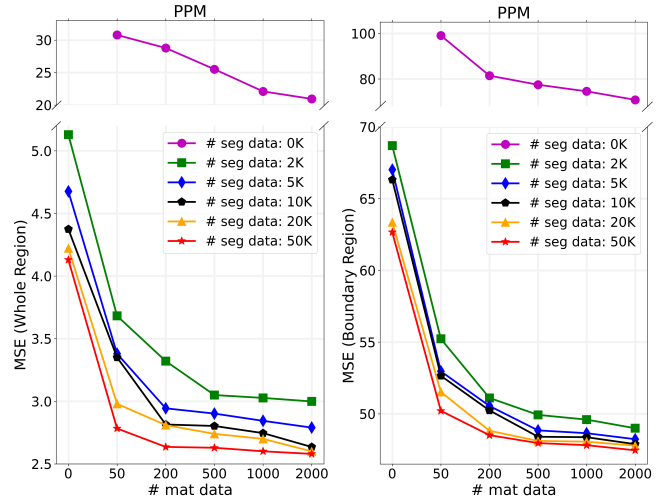


Figure 7. Comparisons on **PPM** dataset (**natural images**) according to the amount of segmentation and matte data.

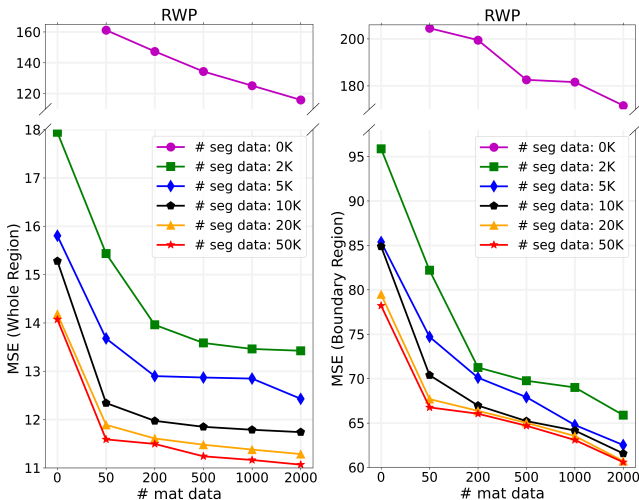


Figure 8. Comparisons on **RWP** dataset (**natural images**) according to the amount of segmentation and matte data.

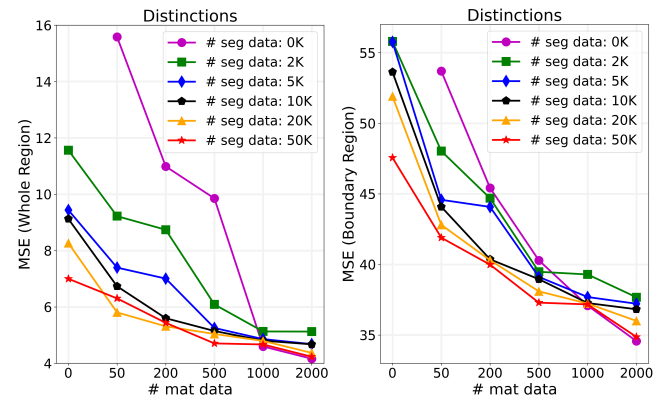


Figure 9. Comparisons on **D-646** dataset (**synthetic images**) according to the amount of segmentation and matte data.

matte data into six subsets with 0, 50, 200, 500, 1000, and 2000 labels. We train the model on all ($=6 \times 6 - 1$) combinations of the segmentation and matte subsets, and evaluate on four validation sets, namely P3M, PPM, RWP, and D-646. We primarily analyze the performance of the model on natural images using P3M (Figure 6), PPM (Figure 7), and RWP (Figure 8) datasets and on synthetic images using D-646 dataset (Figure 9). Note that there is no pre-training for segmentation subsets with zero data counts.

Finding 1: Segmentation data improves the robustness of the matting model to natural images. The model trained with only matte data (*e.g.*, seg 0 & mat 2000) achieves a reasonable performance on synthetic images, as shown in Figure 2c and Figure 9. However, it shows com-

pletely different results on natural images, as shown in Figure 2c and Figures 6–8. The reason is that the model often fails to generalize to natural images because it is trained with only synthetic matte data. When we leverage segmentation data with the proposed training method (*e.g.*, seg 2000 & mat 2000), the performance of the model dramatically improves from 34.2 MSE to 4.1 MSE. We also discover that the performance gap between using 2K and 50K segmentation data is not substantial (4.1 vs. 3.6 MSE). The results demonstrate that (1) domain generalization is a critical issue for trimap-free matting models when training with only synthetic matte data, and (2) although segmentation data consists of weaker information, our method can leverage segmentation data as an effective source to improve the robustness of the model to natural images.

Method	Whole Region MSE ↓				FPS ↑	
	P3M [24]	PPM [19]	RWP [57]	D-646 [42]	GPU	CPU
SHM [6]	40.966	27.306	58.456	23.646	97.0	6.6
GCA [27]	22.176	16.337	32.423	11.523	95.1	5.0
P3MNet [24]	13.586	9.672	24.079	8.935	94.6	11.8
IndexNet [34]	12.484	6.043	20.580	7.683	52.9	1.9
GFM [26]	10.770	5.183	18.895	6.705	100.3	13.3
LFM [60]	9.611	5.970	18.012	6.222	26.3	2.0
MODNet [19]	9.692	5.161	18.038	5.736	101.7	8.9
Ours (R101)	4.391	2.802	11.257	5.301	58.3	5.0
Ours (R18)	7.007	3.518	13.094	6.192	222.2	18.7
Ours (R18 0.5)	8.307	3.996	16.787	7.816	328.9	43.7

Table 1. **Comparison with state-of-the-art trimap-free matting approaches.** All models are trained with the same amount of 10K segmentation and 200 matte labels. The P3M [24], PPM [19], and RWP [57] datasets consist of natural images, and the D-646 [42] consists of synthetic images. The R18 (0.5) denotes UNet ResNet18 backbone network with a width multiplier of 0.5.

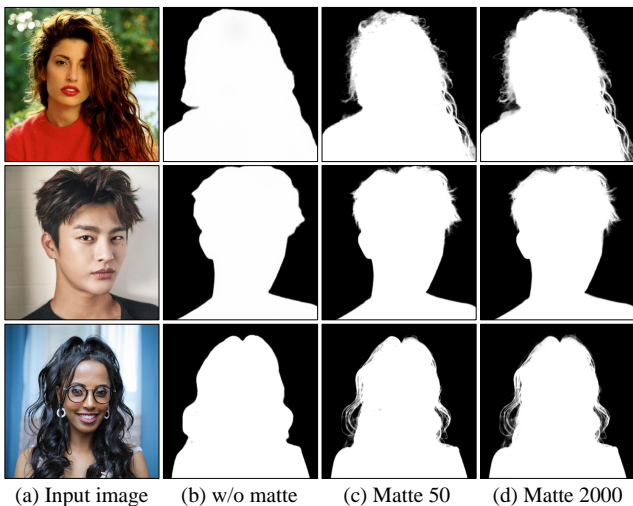


Figure 10. **Qualitative comparisons** according to the amount of matte data with a fixed number of 10K segmentation data: (b) without matte data, (c) 50 matte data, (d) 2000 matte data.

Finding 2: A small amount of matte data can dramatically improve the boundary detail representation of the matting model. The model trained with only segmentation data (*e.g.*, seg 10K & mat 0) performs well on natural images but lacks representing boundary detail information due to the coarse training labels, as shown in Figure 10b. Even when we increase the amount of segmentation data, the improvement of the model in the boundary region is marginal. However, by leveraging a small amount of synthetic matte data, our training method considerably improves the prediction accuracy of the model, especially on the boundary region. As shown in the results on P3M dataset consisting of natural images (Figure 6), the MSE error on the boundary region is steeply decreased when the

amount of matte data is increased from 0 to 50. Moreover, we found that the performance gap between leveraging 50 and 2000 matte data is insignificant, as shown in Figure 10c and Figure 10d. The results demonstrate that (1) incorporating a small amount of matte data using our method can dramatically improve the boundary detail representation of the model, and (2) it gives us more opportunity for cost-efficient human matting using a reduced amount of segmentation and matte data.

Comparison with state-of-the-art methods. Our method is compared to state-of-the-art trimap-free matting methods such as SHM [6], GCA [27], GFM [26], P3MNet [24], IndexNet [34], LFM [60], and MODNet [19] as in Table 1 using the same amount of 10K segmentation and 200 matte labels. Following the training strategy used in [19], all existing methods are pre-trained on segmentation labels and fine-tuned on matte labels. Our three baseline networks are trained using the proposed training method, Matte Label Blending. In addition, we measure the throughput of each model using ONNX runtime [11] on an NVIDIA Tesla V100 GPU and Xeon Gold 5120 CPU with an input size of 512×512 . We evaluate all methods using three real-world datasets (*i.e.*, P3M, PPM, and RWP) consisting of natural images and one synthesized dataset (*i.e.*, D-646) consisting of synthetic images. As a result, the performance of ours on the synthesized dataset is not substantial compared to state-of-the-art matting methods. However, we achieve remarkable performances on real-world datasets since our training method can noticeably improve the domain generalization of the model to natural images. Especially, our training method is successfully applied to the lightweight model (*i.e.*, UNet-ResNet18 with a multiplier of 0.5) achieving extremely fast inference of 328.9 FPS on a GPU and state-of-the-art performance.

Network	Whole Region	Boundary Region
	MSE ↓	MSE ↓
<i>seg 2K, mat 50</i>		
BSHM [32]	20.012	87.186
Context-aware [17]	19.837	52.943
ours	4.901	32.435
<i>seg 10K, mat 200</i>		
BSHM [32]	15.779	80.787
Context-aware [17]	16.844	46.361
ours	4.391	28.776
<i>seg 50K, mat 2000</i>		
BSHM [32]	13.287	75.600
Context-aware [17]	14.092	42.006
ours	3.512	22.728

Table 2. **Comparison with existing training methods**, BSHM [32] and Context-aware [17], for human matting using the same amount of segmentation and matte data.

Also, our training method is compared to existing training methods such as BSHM [32] and Context-aware [17] that are proposed to mitigate the domain generalization issue. We reproduce them using the same amount of segmentation and matte data and evaluate them on P3M validation set. The results in Table 2 demonstrate the substantial superiority of our training method. The reason is that when BSHM sequentially trains three sub-network in an offline manner, the last sub-network is trained with only synthetic matte data, resulting in inevitable domain generalization errors. Also, Context-aware consists of simple image augmentation methods, such as re-JPEGing and Gaussian blur. Such image augmentation may remove some artifacts in synthesized images, but cannot handle the contextual unnaturalness as shown in Figure 1 and Figure 2.

4.4. Analysis

We conduct experiments to analyze each component of our training method on P3M [24] validation set under the segmentation 10K and matte 200 labels setup.

Effect of Matte Label Blending. We compare the performance of the student network with that of the teacher network to investigate the effect of the proposed method. Table 3 and Figure 11 show the comparison results between the student network and two kinds of teacher networks. The first is the teacher network trained with only segmentation data, and the second is the teacher network that is fine-tuned on the synthetic matte data. The teacher network trained with only segmentation data shows a reasonable performance on the whole region, but the boundary detail representation is insufficient, as in Table 3 and Figure 11b. When we fine-tune the teacher network using

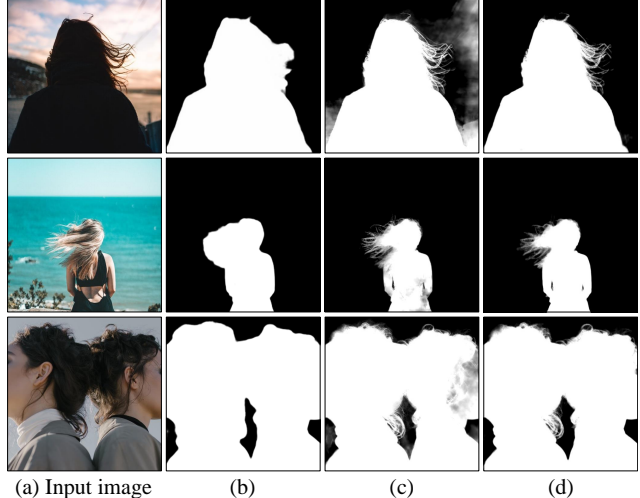


Figure 11. **Qualitative comparisons** under 50K segmentation data and 2K matte data setting: (b) teacher network trained with only segmentation data, (c) teacher network fine-tuned on matte data, (d) student network trained with Matte Label Blending.

Network	Whole Region	Boundary Region
	MSE ↓	MSE ↓
Teacher (seg only)	6.676	48.088
Teacher (fine-tune)	6.991	32.553
Student (ours)	4.391	28.776

Table 3. **Effect of Matte Label Blending.** Note that the Matte Label Blending method is applied only to the student network.

matte data, the boundary detail representation of the network is improved, but there are several noisy predictions in the foreground and background region, dropping the performance in the whole region, as in Table 3 and Figure 11c. When fine-tuning the network, the continuous guiding of synthetic images deteriorates the generalization of the network to natural images. However, the Matte Label Blending is designed to exploit only the advantageous information of the teacher network and segmentation data, and the student network can enjoy a substantial improvement on both the whole and boundary region.

Effect of loss weight λ . We conduct experiments to verify the robustness of the model to the hyperparameter λ used in Eq. 2. The experimental results in Table 4 indicate that our method exhibits consistency across different values of λ . Consequently, we set λ to 0.01 by default, which yields optimal results across our experiments.

λ	Whole Region	Boundary Region
	MSE ↓	MSE ↓
0.1	4.442	28.911
0.01	4.391	28.776
0.001	4.421	28.838

Table 4. **Effect of loss weight λ .** Our training method is robust to changes in λ , and we set λ to 0.01 by default.

Weak-Strong Aug	EMA Update	Whole Region MSE ↓	Boundary Region MSE ↓
✓	✓	4.391	28.776
✓		4.419	28.793
	✓	4.437	28.804
		4.472	28.815

Table 5. **Effect of training strategies: weak-strong augmentation and EMA update.** We follow the detailed setting of them used in teacher-student frameworks [2, 7, 51].

Effect of components in the teacher-student framework.

We designed the baseline training method encompassing teacher-student networks, motivated by [2, 7, 51]. Here, we analyze the effect of weak-strong augmentation and exponential moving average (EMA) update strategies used in the teacher-student framework on the performance of human matting models. The results in Table Tab. 5 indicate that both strategies yield a slight performance improvement. We employ both strategies in our training by default and note that the EMA update is applied only when the teacher and student networks have the same network architecture.

Transferring to existing matting models. Our training method can be easily transferred to existing matting models by changing the student network in Figure 4. We adopt seven existing matting models (SHM [6], MODNet [19], P3MNet [24], GFM [26], GCA [27], IndexNet [34], and LFM [60]) and compare our training method with the fine-tuning technique, where the model is pre-trained on segmentation data and then fine-tuned on matte data. As shown in Table 6, our training method improves the performance of all matting models with a large margin. This result demonstrates that ours can be served as an effective training method to properly incorporate segmentation and matte data. Notably, the state-of-the-art real-time matting model, MODNet, shows an improved performance of 5.602 MSE with a 42.2% reduction in error.

Network	Whole Region	Boundary Region	FPS	
	MSE ↓	MSE ↓	GPU ↑	CPU ↑
UNet-R101	6.991	32.553	58.3	5.0
+ ours	4.472 (−36.0%)	28.837 (−11.4%)		
UNet-R18	9.868	44.735	222.2	18.7
+ ours	7.090 (−28.2%)	30.303 (−32.3%)		
UNet-R18(0.5)	11.388	55.745	328.9	43.7
+ ours	8.335 (−26.8%)	31.059 (−44.3%)		
MODNet [19]	9.692	42.270	101.7	8.9
+ ours	5.655 (−41.7%)	34.335 (−18.8%)		
LFM [60]	9.611	42.737	26.3	2.0
+ ours	6.103 (−36.5%)	29.633 (−30.7%)		
GFM [26]	10.770	43.055	100.3	13.3
+ ours	6.425 (−40.3%)	32.098 (−25.4%)		
P3MNet [24]	13.586	50.146	94.6	11.8
+ ours	7.381 (−45.7%)	35.092 (−30.0%)		
IndexNet [34]	12.484	46.936	52.9	1.9
+ ours	7.554 (−39.5%)	34.596 (−26.3%)		
GCA [27]	22.176	65.232	95.1	5.0
+ ours	8.875 (−60.0%)	36.712 (−43.7%)		
SHM [6]	40.966	106.338	97.01	6.6
+ ours	19.073 (−53.4%)	46.899 (−52.0%)		

Table 6. **Transferring our training method to existing matting networks.** +ours denotes that the network is trained as the student network in our training method. Otherwise, the network is pre-trained on the same amount of 10K segmentation data and then fine-tuned on the same amount of 200 matte data. The models are evaluated on P3M [24] dataset.

5. Conclusion and Future Direction

In this paper, we introduced a new practical learning setting for human matting that utilizes both relatively easy-to-find coarse segmentation data and precise but expensive matte data. Firstly, We observed that the segmentation data contains coarse-level human region information, and the model trained with matte data captures delicate details information mainly in the boundary region. Based on the observation, the proposed Matte Label Blending method showed that guiding only informative knowledge from segmentation data and the model trained with matte data makes the matting model robust to natural images and precise boundary detail representation. From the extensive experiments, we analyzed the effect of the amount of segmentation and matte data for human matting and verified the effectiveness of the proposed method. Although we showed the segmentation data could be effectively used in human matting, we have a limit in the comfortable usability of an extensive pool of unlabeled images, such as web-crawling images. Our promising future research direction will be applying pseudo-segmentation labels to utilize a huge amount of unlabeled images in the proposed framework.

References

- [1] Supervisely person dataset. <https://supervisely.com/explore/projects/supervisely-person-dataset-23304/datasets>. Accessed: 2022-09-01. 4
- [2] David Berthelot, Nicholas Carlini, Ian Goodfellow, Nicolas Papernot, Avital Oliver, and Colin A Raffel. Mixmatch: A holistic approach to semi-supervised learning. *Advances in neural information processing systems*, 32, 2019. 4, 9
- [3] Shaofan Cai, Xiaoshuai Zhang, Haoqiang Fan, Haibin Huang, Jiangyu Liu, Jiaming Liu, Jiaying Liu, Jue Wang, and Jian Sun. Disentangled image matting. In *Proceedings of the IEEE/CVF International Conference on Computer Vision*, pages 8819–8828, 2019.
- [4] Liangyu Chen, Tong Yang, Xiangyu Zhang, Wei Zhang, and Jian Sun. Points as queries: Weakly semi-supervised object detection by points. In *Proceedings of the IEEE/CVF Conference on Computer Vision and Pattern Recognition*, pages 8823–8832, 2021. 3
- [5] Liang-Chieh Chen, George Papandreou, Iasonas Kokkinos, Kevin Murphy, and Alan L Yuille. Deeplab: Semantic image segmentation with deep convolutional nets, atrous convolution, and fully connected crfs. *IEEE transactions on pattern analysis and machine intelligence*, 40(4):834–848, 2017. 5, 14
- [6] Quan Chen, Tiezheng Ge, Yanyu Xu, Zhiqiang Zhang, Xinxin Yang, and Kun Gai. Semantic human matting. In *Proceedings of the 26th ACM international conference on Multimedia*, pages 618–626, 2018. 1, 3, 5, 7, 9
- [7] Ting Chen, Simon Kornblith, Mohammad Norouzi, and Geoffrey Hinton. A simple framework for contrastive learning of visual representations. In *International conference on machine learning*, pages 1597–1607. PMLR, 2020. 4, 5, 9
- [8] Hang Cheng, Shugong Xu, Xiufeng Jiang, and Rongrong Wang. Deep image matting with flexible guidance input. *arXiv preprint arXiv:2110.10898*, 2021.
- [9] Donghyeon Cho, Yu-Wing Tai, and Inso Kweon. Natural image matting using deep convolutional neural networks. In *European Conference on Computer Vision*, pages 626–643. Springer, 2016. 1, 3
- [10] Yutong Dai, Brian Price, He Zhang, and Chunhua Shen. Boosting robustness of image matting with context assembling and strong data augmentation. In *Proceedings of the IEEE/CVF Conference on Computer Vision and Pattern Recognition*, pages 11707–11716, 2022.
- [11] ONNX Runtime developers. Onnx runtime. <https://onnxruntime.ai/>, 2021. Version: x.y.z. 7
- [12] Alexey Dosovitskiy, Lucas Beyer, Alexander Kolesnikov, Dirk Weissenborn, Xiaohua Zhai, Thomas Unterthiner, Mostafa Dehghani, Matthias Minderer, Georg Heigold, Sylvain Gelly, et al. An image is worth 16x16 words: Transformers for image recognition at scale. *arXiv preprint arXiv:2010.11929*, 2020. 3
- [13] Mark Everingham, Luc Van Gool, Christopher KI Williams, John Winn, and Andrew Zisserman. The pascal visual object classes (voc) challenge. *International journal of computer vision*, 88(2):303–338, 2010. 5
- [14] Shijie Fang, Yuhang Cao, Xinjiang Wang, Kai Chen, Dahua Lin, and Wayne Zhang. Wssod: A new pipeline for weakly-and semi-supervised object detection. *arXiv preprint arXiv:2105.11293*, 2021. 3
- [15] Marco Forte and François Pitié. f, b , alpha matting. *arXiv preprint arXiv:2003.07711*, 2020.
- [16] Kaiming He, Xiangyu Zhang, Shaoqing Ren, and Jian Sun. Deep residual learning for image recognition. In *Proceedings of the IEEE conference on computer vision and pattern recognition*, pages 770–778, 2016. 5, 13, 14
- [17] Qiqi Hou and Feng Liu. Context-aware image matting for simultaneous foreground and alpha estimation. In *Proceedings of the IEEE/CVF International Conference on Computer Vision*, pages 4130–4139, 2019. 8
- [18] Yasamin Jafarian and Hyun Soo Park. Learning high fidelity depths of dressed humans by watching social media dance videos. In *Proceedings of the IEEE/CVF Conference on Computer Vision and Pattern Recognition*, pages 12753–12762, 2021. 4
- [19] Zhanghan Ke, Jiayu Sun, Kaican Li, Qiong Yan, and Rynson WH Lau. Modnet: Real-time trimap-free portrait matting via objective decomposition. In *Proceedings of the AAAI Conference on Artificial Intelligence*, pages 1140–1147, 2022. 1, 3, 4, 7, 9, 14
- [20] Beomyoung Kim, Sangeun Han, and Junmo Kim. Discriminative region suppression for weakly-supervised semantic segmentation. In *Proceedings of the AAAI Conference on Artificial Intelligence*, pages 1754–1761, 2021.
- [21] Beomyoung Kim, Youngjoon Yoo, Chae Eun Rhee, and Junmo Kim. Beyond semantic to instance segmentation: Weakly-supervised instance segmentation via semantic knowledge transfer and self-refinement. In *Proceedings of the IEEE/CVF Conference on Computer Vision and Pattern Recognition*, pages 4278–4287, 2022.
- [22] Beomyoung Kim, Joonhyun Jeong, Dongyoon Han, and Sung Ju Hwang. The devil is in the points: Weakly semi-supervised instance segmentation via point-guided mask representation. In *Proceedings of the IEEE/CVF Conference on Computer Vision and Pattern Recognition*, pages 11360–11370, 2023. 3
- [23] Jungbeom Lee, Eunji Kim, and Sungroh Yoon. Anti-adversarially manipulated attributions for weakly and semi-supervised semantic segmentation. In *Proceedings of the IEEE/CVF Conference on Computer Vision and Pattern Recognition*, pages 4071–4080, 2021.
- [24] Jizhizi Li, Sihan Ma, Jing Zhang, and Dacheng Tao. Privacy-preserving portrait matting. In *Proceedings of the 29th ACM International Conference on Multimedia*, pages 3501–3509, 2021. 4, 7, 8, 9, 14
- [25] Jizhizi Li, Jing Zhang, and Dacheng Tao. Deep automatic natural image matting. In *Proceedings of the Thirtieth International Joint Conference on Artificial Intelligence, IJCAI-21*, pages 800–806, 2021.
- [26] Jizhizi Li, Jing Zhang, Stephen J Maybank, and Dacheng Tao. Bridging composite and real: towards end-to-end deep image matting. *International Journal of Computer Vision*, 130(2):246–266, 2022. 7, 9

- [27] Yaoyi Li and Hongtao Lu. Natural image matting via guided contextual attention. In *Proceedings of the AAAI Conference on Artificial Intelligence*, pages 11450–11457, 2020. 7, 9
- [28] Shanchuan Lin, Andrey Ryabtsev, Soumyadip Sengupta, Brian L Curless, Steven M Seitz, and Ira Kemelmacher-Shlizerman. Real-time high-resolution background matting. In *Proceedings of the IEEE/CVF Conference on Computer Vision and Pattern Recognition*, pages 8762–8771, 2021.
- [29] Shanchuan Lin, Linjie Yang, Imran Saleemi, and Soumyadip Sengupta. Robust high-resolution video matting with temporal guidance. In *Proceedings of the IEEE/CVF Winter Conference on Applications of Computer Vision*, pages 238–247, 2022.
- [30] Tsung-Yi Lin, Michael Maire, Serge Belongie, James Hays, Pietro Perona, Deva Ramanan, Piotr Dollár, and C Lawrence Zitnick. Microsoft coco: Common objects in context. In *European conference on computer vision*, pages 740–755. Springer, 2014. 4
- [31] Chang Liu, Henghui Ding, and Xudong Jiang. Towards enhancing fine-grained details for image matting. In *Proceedings of the IEEE/CVF Winter Conference on Applications of Computer Vision*, pages 385–393, 2021.
- [32] Jinlin Liu, Yuan Yao, Wendi Hou, Miaomiao Cui, Xuansong Xie, Changshui Zhang, and Xian-sheng Hua. Boosting semantic human matting with coarse annotations. In *Proceedings of the IEEE/CVF Conference on Computer Vision and Pattern Recognition*, pages 8563–8572, 2020. 3, 8
- [33] Yuhao Liu, Jiake Xie, Xiao Shi, Yu Qiao, Yujie Huang, Yong Tang, and Xin Yang. Tripartite information mining and integration for image matting. In *Proceedings of the IEEE/CVF International Conference on Computer Vision*, pages 7555–7564, 2021. 1, 3, 4, 5
- [34] Hao Lu, Yutong Dai, Chunhua Shen, and Songcen Xu. Indices matter: Learning to index for deep image matting. In *Proceedings of the IEEE/CVF International Conference on Computer Vision*, pages 3266–3275, 2019. 1, 3, 7, 9
- [35] Sebastian Lutz, Konstantinos Amplianitis, and Aljosa Smolic. Alphagan: Generative adversarial networks for natural image matting. *arXiv preprint arXiv:1807.10088*, 2018.
- [36] George Papandreou, Liang-Chieh Chen, Kevin P Murphy, and Alan L Yuille. Weakly-and semi-supervised learning of a deep convolutional network for semantic image segmentation. In *Proceedings of the IEEE international conference on computer vision*, pages 1742–1750, 2015.
- [37] GyuTae Park, SungJoon Son, JaeYoung Yoo, SeHo Kim, and Nojun Kwak. Matteformer: Transformer-based image matting via prior-tokens. In *Proceedings of the IEEE/CVF Conference on Computer Vision and Pattern Recognition*, pages 11696–11706, 2022. 1, 3, 4
- [38] Hyojin Park, Lars Lowe Sjöstrand, YoungJoon Yoo, Jihwan Bang, and Nojun Kwak. Extremec3net: extreme lightweight portrait segmentation networks using advanced c3-modules. *arXiv preprint arXiv:1908.03093*, 2019.
- [39] Hyojin Park, Lars Sjosund, YoungJoon Yoo, Nicolas Monet, Jihwan Bang, and Nojun Kwak. Sinet: Extreme lightweight portrait segmentation networks with spatial squeeze module and information blocking decoder. In *Proceedings of the IEEE/CVF Winter Conference on Applications of Computer Vision*, pages 2066–2074, 2020.
- [40] Kwanyong Park, Sanghyun Woo, Seoung Wug Oh, In So Kweon, and Joon-Young Lee. Mask-guided matting in the wild. In *Proceedings of the IEEE/CVF Conference on Computer Vision and Pattern Recognition*, pages 1992–2001, 2023. 3
- [41] Adam Paszke, Sam Gross, Francisco Massa, Adam Lerer, James Bradbury, Gregory Chanan, Trevor Killeen, Zeming Lin, Natalia Gimelshein, Luca Antiga, et al. Pytorch: An imperative style, high-performance deep learning library. *Advances in neural information processing systems*, 32, 2019. 5
- [42] Yu Qiao, Yuhao Liu, Xin Yang, Dongsheng Zhou, Mingliang Xu, Qiang Zhang, and Xiaopeng Wei. Attention-guided hierarchical structure aggregation for image matting. In *Proceedings of the IEEE/CVF Conference on Computer Vision and Pattern Recognition*, pages 13676–13685, 2020. 1, 3, 4, 5, 7, 14
- [43] Olaf Ronneberger, Philipp Fischer, and Thomas Brox. U-net: Convolutional networks for biomedical image segmentation. In *International Conference on Medical image computing and computer-assisted intervention*, pages 234–241. Springer, 2015. 5, 13, 14
- [44] Soumyadip Sengupta, Vivek Jayaram, Brian Curless, Steven M Seitz, and Ira Kemelmacher-Shlizerman. Background matting: The world is your green screen. In *Proceedings of the IEEE/CVF Conference on Computer Vision and Pattern Recognition*, pages 2291–2300, 2020.
- [45] Hongje Seong, Seoung Wug Oh, Brian Price, Euntai Kim, and Joon-Young Lee. One-trimap video matting. In *Computer Vision—ECCV 2022: 17th European Conference, Tel Aviv, Israel, October 23–27, 2022, Proceedings, Part XXIX*, pages 430–448. Springer, 2022.
- [46] Xiaoyong Shen, Aaron Hertzmann, Jiaya Jia, Sylvain Paris, Brian Price, Eli Shechtman, and Ian Sachs. Automatic portrait segmentation for image stylization. In *Computer Graphics Forum*, pages 93–102. Wiley Online Library, 2016. 4
- [47] Xiaoyong Shen, Xin Tao, Hongyun Gao, Chao Zhou, and Jiaya Jia. Deep automatic portrait matting. In *European conference on computer vision*, pages 92–107. Springer, 2016. 1, 3
- [48] Yanan Sun, Chi-Keung Tang, and Yu-Wing Tai. Semantic image matting. In *Proceedings of the IEEE/CVF Conference on Computer Vision and Pattern Recognition*, pages 11120–11129, 2021.
- [49] Yanan Sun, Guanzhi Wang, Qiao Gu, Chi-Keung Tang, and Yu-Wing Tai. Deep video matting via spatio-temporal alignment and aggregation. In *Proceedings of the IEEE/CVF Conference on Computer Vision and Pattern Recognition*, pages 6975–6984, 2021.
- [50] Jingwei Tang, Yagiz Aksoy, Cengiz Oztireli, Markus Gross, and Tunc Ozan Aydin. Learning-based sampling for natural image matting. In *Proceedings of the IEEE/CVF Conference on Computer Vision and Pattern Recognition*, pages 3055–3063, 2019. 1, 3
- [51] Antti Tarvainen and Harri Valpola. Mean teachers are better role models: Weight-averaged consistency targets improve

- semi-supervised deep learning results. *Advances in neural information processing systems*, 30, 2017. 4, 9
- [52] Tianyi Wei, Dongdong Chen, Wenbo Zhou, Jing Liao, Hanqing Zhao, Weiming Zhang, and Nenghai Yu. Improved image matting via real-time user clicks and uncertainty estimation. In *Proceedings of the IEEE/CVF Conference on Computer Vision and Pattern Recognition*, pages 15374–15383, 2021.
- [53] Zifeng Wu, Yongzhen Huang, Yinan Yu, Liang Wang, and Tieniu Tan. Early hierarchical contexts learned by convolutional networks for image segmentation. In *2014 22nd International Conference on Pattern Recognition*, pages 1538–1543. IEEE, 2014. 4
- [54] Ning Xu, Brian Price, Scott Cohen, and Thomas Huang. Deep image matting. In *CVPR*, 2017. 1, 3
- [55] Ziang Yan, Jian Liang, Weishen Pan, Jin Li, and Changshui Zhang. Weakly-and semi-supervised object detection with expectation-maximization algorithm. *arXiv preprint arXiv:1702.08740*, 2017. 3
- [56] Haichao Yu, Ning Xu, Zilong Huang, Yuqian Zhou, and Humphrey Shi. High-resolution deep image matting. In *Proceedings of the AAAI Conference on Artificial Intelligence*, pages 3217–3224, 2021.
- [57] Qihang Yu, Jianming Zhang, He Zhang, Yilin Wang, Zhe Lin, Ning Xu, Yutong Bai, and Alan Yuille. Mask guided matting via progressive refinement network. In *Proceedings of the IEEE/CVF Conference on Computer Vision and Pattern Recognition*, pages 1154–1163, 2021. 1, 3, 4, 5, 7, 14
- [58] Shilong Zhang, Zhuoran Yu, Liyang Liu, Xinjiang Wang, Aojun Zhou, and Kai Chen. Group r-cnn for weakly semi-supervised object detection with points. In *Proceedings of the IEEE/CVF Conference on Computer Vision and Pattern Recognition*, pages 9417–9426, 2022. 3
- [59] Song-Hai Zhang, Xin Dong, Hui Li, Ruilong Li, and Yong-Liang Yang. Portraitnet: Real-time portrait segmentation network for mobile device. *Computers & Graphics*, 80:104–113, 2019.
- [60] Yunke Zhang, Lixue Gong, Lubin Fan, Peiran Ren, Qixing Huang, Hujun Bao, and Weiwei Xu. A late fusion cnn for digital matting. In *Proceedings of the IEEE/CVF conference on computer vision and pattern recognition*, pages 7469–7478, 2019. 1, 3, 4, 5, 7, 9
- [61] Yijie Zhong, Bo Li, Lv Tang, Hao Tang, and Shouhong Ding. Highly efficient natural image matting. *arXiv preprint arXiv:2110.12748*, 2021.
- [62] Bingke Zhu, Yingying Chen, Jinqiao Wang, Si Liu, Bo Zhang, and Ming Tang. Fast deep matting for portrait animation on mobile phone. In *Proceedings of the 25th ACM international conference on Multimedia*, pages 297–305, 2017. 3

Appendix

A. Additional Analysis

A.1. Network architecture

As mentioned in the experiment section, we used the U-Net [43] structure with ResNet [16] backbone network. In Figure 12, we provide an illustration of our network architecture. Note that we remove the max-pooling layer in the stem part of the ResNet, and the architecture is highly straightforward and simple.

A.2. Detailed quantitative results

In Figures 5–8, we provided the quantitative scores of the matting model according to the amounts of segmentation and matte data in the form of a graph. Here, we provide all numerical scores including MSE and SAD metrics in Table 7.

A.3. Additional Qualitative results

We provide more additional qualitative results in Figure 13; compared to the models trained with only segmentation data or matte data, the model with the proposed method shows more robust results on natural images with finer boundary details.

# seg	# mat	Natural Images										Synthetic Images					
		PPM [19]				P3M [24]				RWP [57]				Distinctions-646 [42]			
		Whole Region		Boundary Region		Whole Region		Boundary Region		Whole Region		Boundary Region		Whole Region		Boundary Region	
		MSE ↓	SAD ↓	MSE ↓	SAD ↓	MSE ↓	SAD ↓	MSE ↓	SAD ↓	MSE ↓	SAD ↓	MSE ↓	SAD ↓	MSE ↓	SAD ↓		
2K	0	5.129	154.675	68.699	65.668	6.907	29.991	50.727	15.329	17.943	50.777	95.872	28.608	11.562	99.361	55.793	46.424
5K	0	4.676	137.027	67.019	65.649	6.771	29.534	50.401	14.347	15.805	49.369	85.372	27.676	9.438	92.097	55.769	46.407
10K	0	4.375	124.083	66.326	64.557	6.676	28.158	48.088	14.077	15.279	48.191	84.883	28.969	9.125	90.853	53.630	45.329
20K	0	4.222	114.015	63.351	64.356	6.539	26.152	45.760	13.822	14.185	47.283	79.485	28.041	8.265	89.945	51.904	44.767
50K	0	4.130	102.522	62.662	64.186	6.493	26.113	43.031	13.577	14.072	46.108	78.211	27.845	7.001	80.785	47.563	43.558
0	50	30.781	532.989	99.097	78.266	50.220	137.725	93.092	21.302	161.199	180.452	204.548	43.815	15.584	99.183	53.696	47.369
2K	50	3.682	82.504	55.228	56.894	4.994	21.080	32.558	10.867	15.435	44.122	82.191	25.885	9.222	68.998	48.033	41.664
5K	50	3.380	81.419	52.964	55.520	4.764	20.824	31.519	10.723	13.678	42.349	74.699	24.994	7.397	58.224	44.578	40.306
10K	50	3.351	78.560	52.651	54.914	4.629	19.768	30.698	10.578	12.342	41.685	70.383	24.982	6.734	55.813	44.084	40.088
20K	50	2.980	74.714	51.526	53.537	4.593	19.132	29.871	10.499	11.891	41.277	67.690	24.855	5.808	55.055	42.805	39.580
50K	50	2.783	71.655	50.211	52.907	4.512	18.764	28.368	10.141	11.590	40.995	66.759	24.746	6.304	52.233	41.897	37.967
0	200	28.778	379.350	81.467	74.051	38.322	125.955	71.315	19.607	147.368	174.427	199.475	43.181	12.986	67.594	42.418	38.423
2K	200	3.321	77.307	51.109	54.613	4.743	19.943	30.573	10.423	13.960	35.479	71.251	25.117	8.739	58.641	44.689	40.136
5K	200	2.944	74.930	50.548	54.057	4.569	18.909	29.781	10.208	12.899	33.820	70.103	24.939	7.007	54.526	44.076	39.143
10K	200	2.815	72.908	50.240	53.624	4.472	18.392	28.837	10.168	11.974	32.871	66.965	24.905	5.601	54.049	40.366	38.530
20K	200	2.810	72.801	48.821	52.648	4.408	18.114	28.016	10.079	11.609	32.567	66.367	24.726	5.314	49.867	40.302	37.971
50K	200	2.636	70.763	48.512	52.112	4.303	17.755	27.900	10.027	11.496	31.173	66.044	24.589	5.438	49.512	39.985	37.144
0	500	25.513	358.315	77.480	65.381	36.656	97.700	69.166	16.868	134.276	172.330	182.532	40.766	11.852	46.528	40.290	35.524
2K	500	3.027	74.792	49.926	53.972	4.466	17.443	27.981	10.128	13.585	35.452	69.758	25.099	6.090	48.846	39.481	37.218
5K	500	2.902	73.733	48.846	52.937	4.260	16.975	27.691	9.991	12.870	33.499	67.908	24.900	5.255	48.753	39.117	36.762
10K	500	2.803	72.889	48.402	52.550	4.198	16.766	27.136	9.703	11.850	32.512	65.216	24.641	5.148	47.151	38.955	36.539
20K	500	2.740	71.639	48.111	52.075	4.073	16.681	25.541	9.635	11.480	32.417	65.016	24.573	5.043	46.847	38.095	36.320
50K	500	2.629	68.218	47.961	51.970	3.965	16.287	25.880	9.629	11.240	30.868	64.692	24.561	4.707	46.422	37.293	35.635
0	1000	22.102	278.938	74.582	62.741	36.123	92.371	62.685	15.423	125.071	162.275	181.543	40.163	4.598	45.086	37.086	35.213
2K	1000	3.050	71.727	49.598	53.074	4.316	16.402	27.052	9.967	13.461	35.382	69.004	25.062	5.131	47.592	39.291	36.588
5K	1000	2.844	70.688	48.650	51.962	4.074	16.371	26.943	9.836	12.848	32.988	64.773	24.786	4.860	47.473	37.692	35.889
10K	1000	2.746	70.187	48.370	51.928	3.979	16.002	25.837	9.517	11.789	31.406	64.149	24.532	4.805	45.857	37.265	35.865
20K	1000	2.700	68.380	48.060	51.918	3.766	15.974	24.663	9.511	11.379	31.311	63.536	24.525	4.795	45.494	37.230	35.618
50K	1000	2.601	67.634	47.813	51.553	3.695	15.562	24.556	9.455	11.164	30.734	63.085	24.310	4.670	45.368	37.172	35.612
0	2000	20.950	224.514	62.836	54.350	33.823	86.223	57.339	14.822	115.815	140.533	171.560	39.019	4.163	42.115	34.568	34.568
2K	2000	2.999	69.131	48.994	51.501	4.076	16.283	25.130	9.840	13.424	35.309	65.878	24.997	5.127	46.936	37.674	35.953
5K	2000	2.790	67.960	48.232	51.312	3.949	15.836	24.030	9.654	12.430	32.831	62.515	24.683	4.682	46.478	37.218	35.756
10K	2000	2.635	67.876	47.886	51.451	3.760	15.823	23.906	9.412	11.740	31.215	61.568	24.511	4.674	45.535	36.826	35.372
20K	2000	2.600	67.350	47.781	51.071	3.634	14.757	22.853	9.404	11.286	30.624	60.714	24.489	4.371	44.567	36.000	35.322
50K	2000	2.580	66.081	47.457	50.963	3.594	14.516	22.831	9.301	11.067	30.025	60.580	24.164	4.234	42.929	34.866	34.755

Table 7. The whole numerical scores of our model on three validation sets consisting of natural images (PPM [19], P3M [24], and RWP [57]) and one synthetic validation set (Distinctions-646 [42]) according to the amounts of segmentation and matte data.

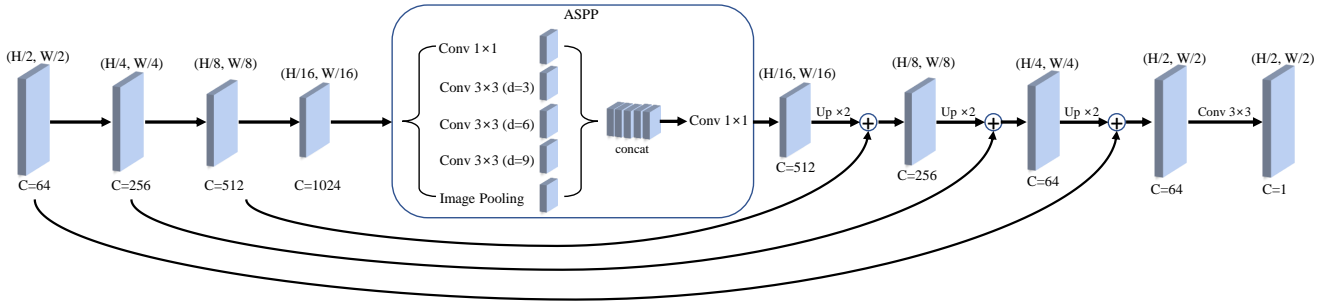


Figure 12. **Illustration of the network architecture we used.** We adopt the U-Net [43] based architecture with the ResNet [16] backbone network and ASPP module [5]. Conv 3×3 (d=3) means using a convolutional neural network with the kernel size of 3×3 and the dilation rate of 3. Up $\times 2$ means applying a bilinear upsampling layer.

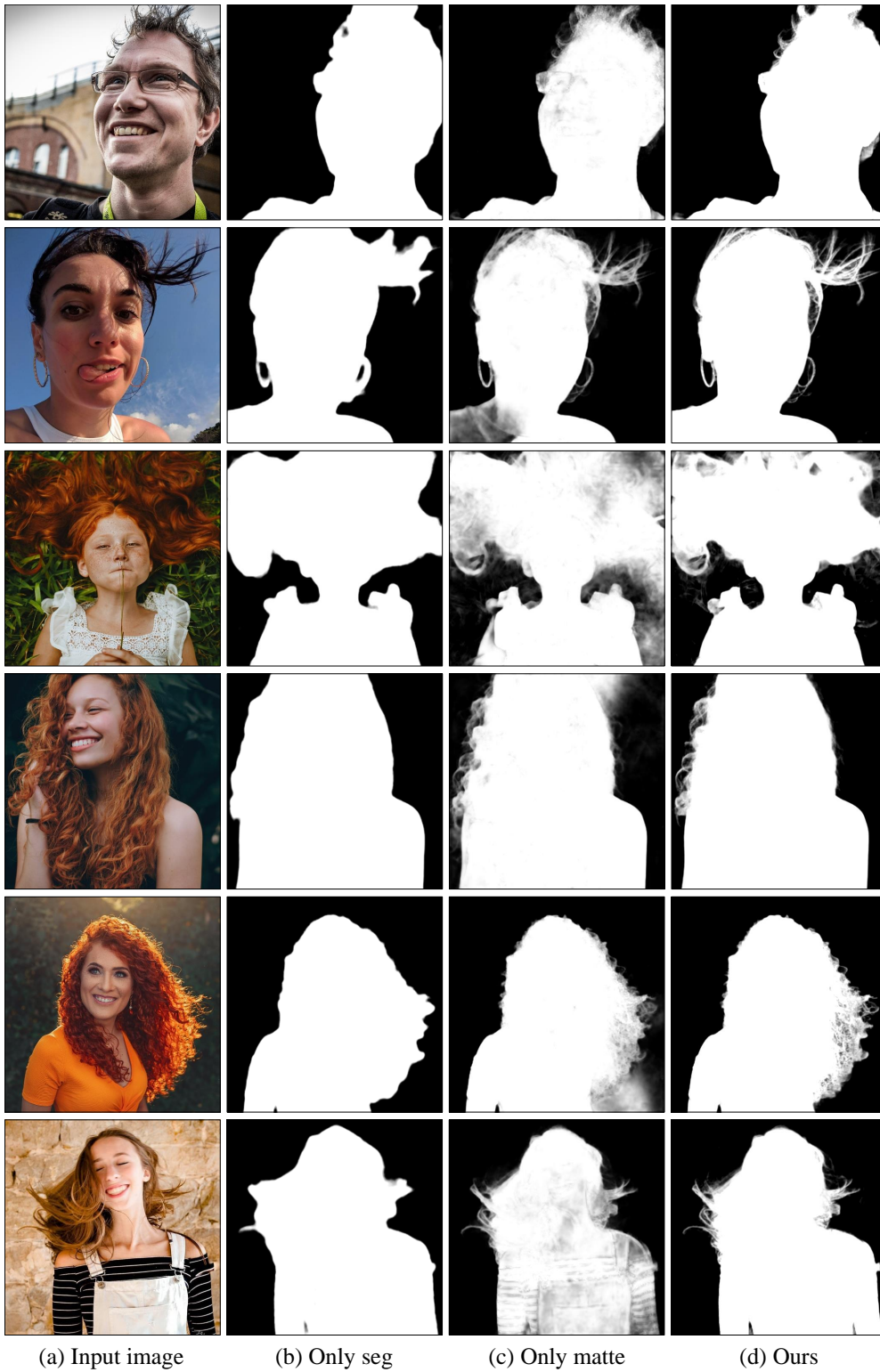


Figure 13. **Additional qualitative comparisons for the models:** the model trained with (b) only segmentation data, (c) only matte data, (d) and both segmentation and matte data with our training method.